Supporting Information

Study of ferro- and anti- ferroelectric polar order in mesophases exhibited by bent-core mesogens

Susanta Chakraborty,[a] Malay Kumar Das,*[a] Christina Keith[b] and Carsten Tschierske[b]

[a] *Department of Physics, North Bengal University, Siliguri-734 013, India*
[b] *Martin-Luther-Universität Halle-Wittenberg, Institut für Chemie, Physikalische Chemie, Halle, Germany*
E-mail: mkdnbu@yahoo.com

1. Dielectric spectroscopy calculations

In order to understand the nature of the dielectric relaxation modes, the frequency-dependent dielectric loss $\varepsilon''(f)$ curves have been fitted by Havriliak-Negami (H-N) fit function with an additional term standing for the low-frequency conductivity contribution as follows:

$$\varepsilon'' = \frac{\sigma_0}{(2\pi f)^S} + \sum_{k=1}^{N} \frac{\delta\varepsilon_k \sin(\beta\theta)}{[1+(2\pi f \tau_k)^{2\alpha_k} + 2(2\pi f \tau_k)^{\alpha_k}\cos(\alpha_k \pi/2)]^{\beta/2}} \qquad (1)$$

with $\theta = \tan^{-1}\left[\frac{(2\pi f \tau_k)^{\alpha_k}\sin(\alpha_k\pi/2)}{1+(2\pi f\tau_k)^{\alpha_k}\cos(\alpha_k\pi/2)}\right]$

where $\delta\varepsilon_k$ is the dielectric strength, ε_∞ is the high-frequency limit of the permittivity, τ_k (= $1/2\pi f_k$) is the relaxation time, f_k is the corresponding relaxation frequency, α_k and β_k are the shape parameters (can be between 0 and 1) describing the symmetric and non-symmetric broadness of dielectric dispersion curve, respectively and k is the number of relaxation processes. However, σ_0 is related to the DC conductivity and S is a fitting parameter responsible for the slope of the conductivity.

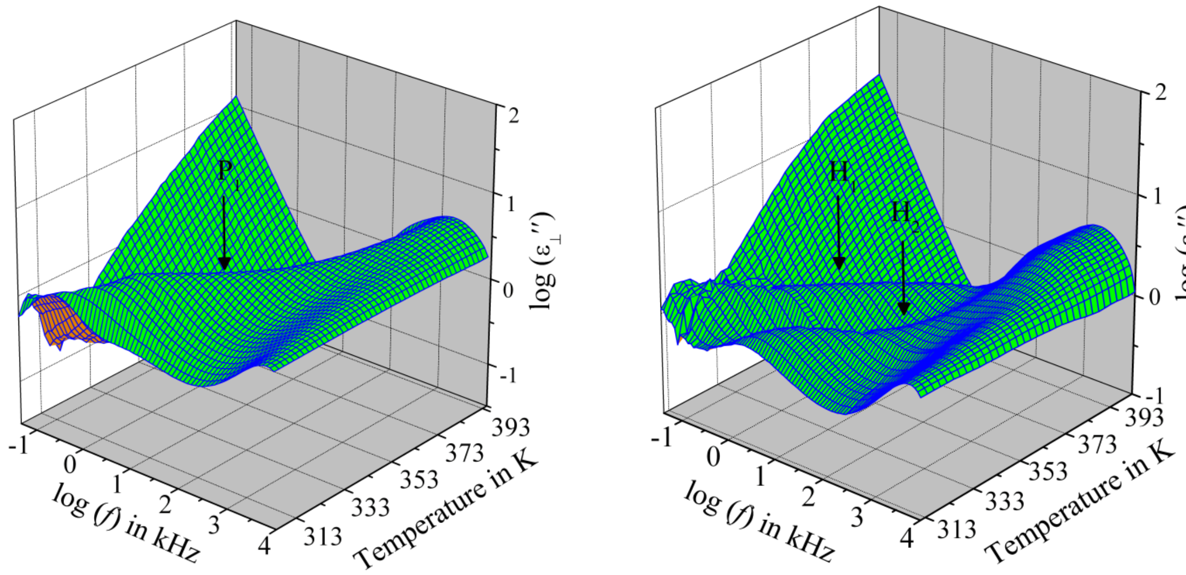

(a) (b)

Figure S1. Frequency dependence of the imaginary (ε'') parts of the permittivity at different temperatures for compound **1/7:** in (a) HG or planar and (b) HT or homeotropic sample configurations.

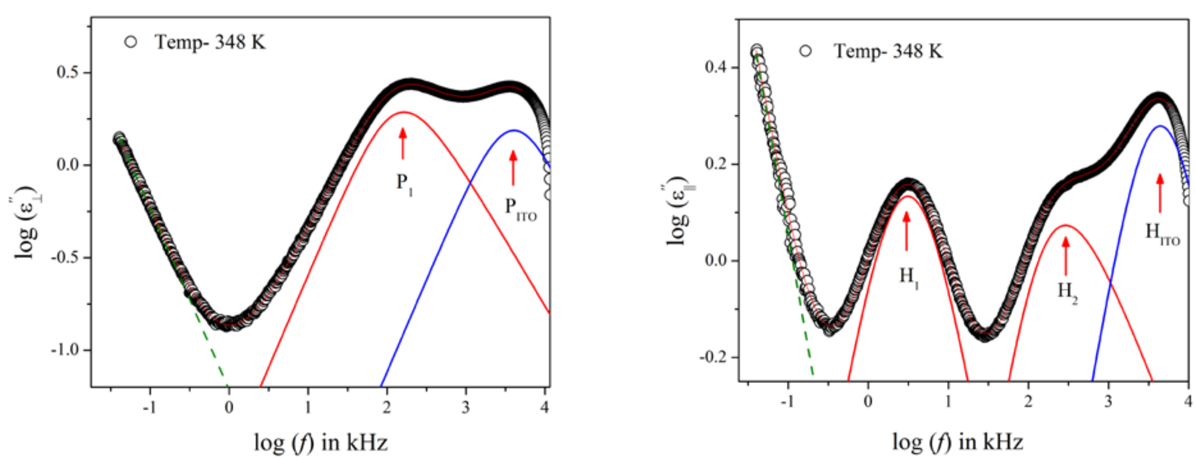

(a) (b)

Figure S2. Frequency dependence of imaginary (ε'') parts of permittivity for the compound **1/7** at a particular temperature: in (a) HG or planar and (b) HT or homeotropic sample configurations. Solid curves represent different relaxation modes obtained after fit to data points with H-N equation.

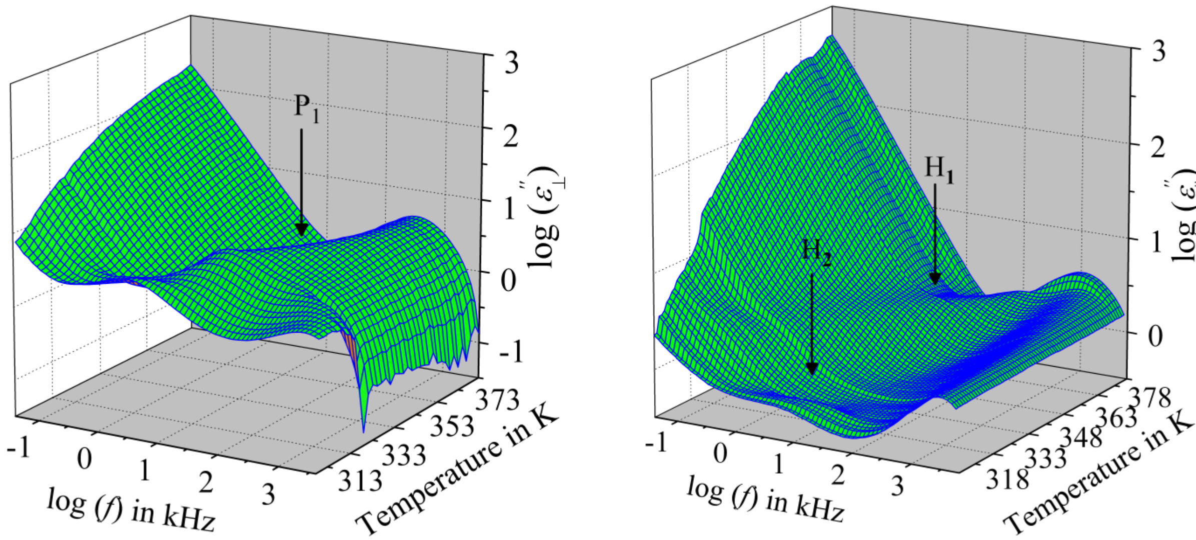

(a) (b)

Figure S3. Frequency dependence of the imaginary (ε'') parts of the permittivity at different temperatures for compound **1/9:** in (a) HG or planar and (b) HT or homeotropic sample configurations.

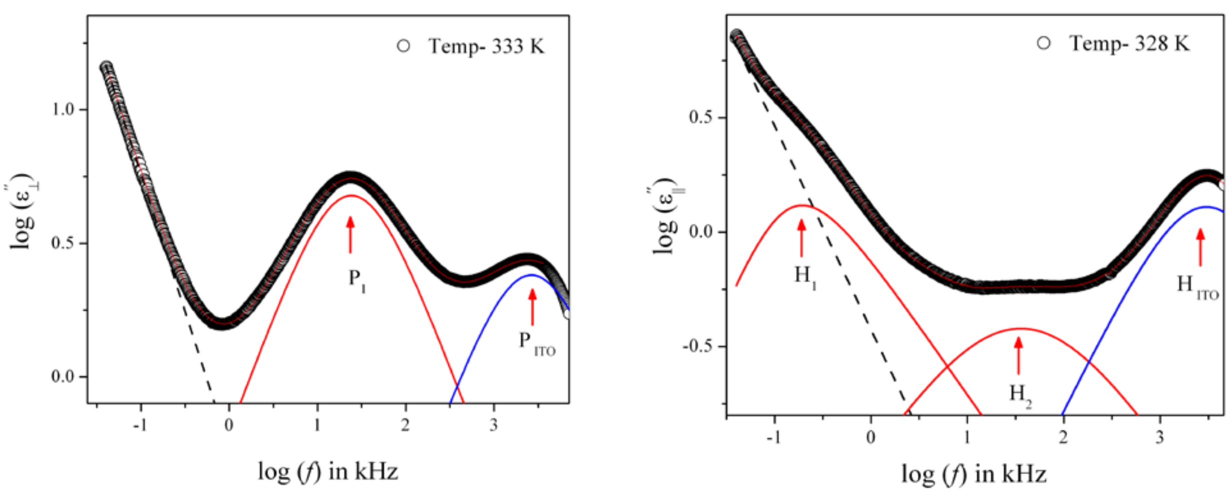

(a) (b)

Figure S4. Frequency dependence of imaginary (ε'') parts of permittivity for the compound **1/9** at a particular temperature**:** in (a) HG or planar and (b) HT or homeotropic sample configurations. Solid curves represent different relaxation modes obtained after fit to data points with H-N equation.

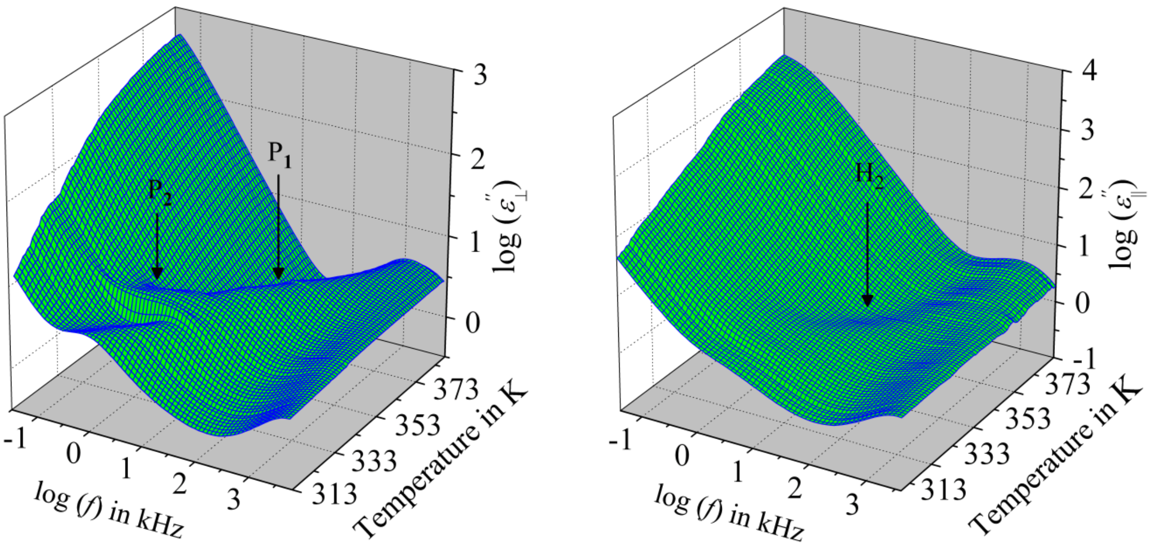

(a) (b)

Figure S5. Frequency dependence of the imaginary (ε'') parts of the complex permittivity at different temperatures for compound **1/10**: in (a) planar and (b) homeotropic oriented samples.

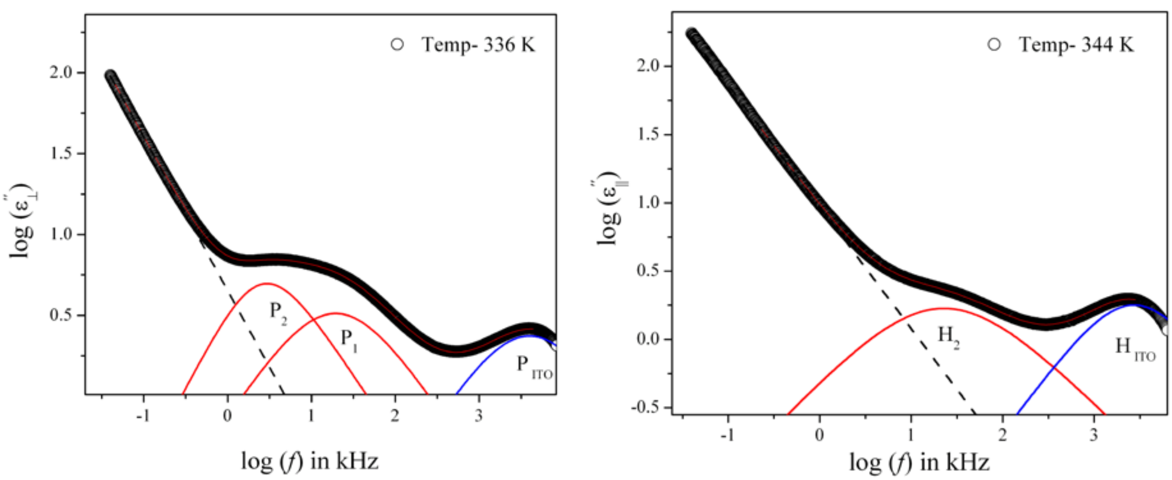

(a) (b)

Figure S6. Frequency dependence of imaginary (ε'') parts of permittivity for the compound **1/10** at a particular temperature**:** in (a) HG or planar and (b) HT or homeotropic sample configurations. Solid curves represent different relaxation modes obtained after fit to data points with H-N equation.

3. Electro-optical study

With an application of an square wave of voltage 180 V_{PP} and frequency 5 Hz, the optical textures were observed in ITO coated cells with planar and homeotropic alignments.

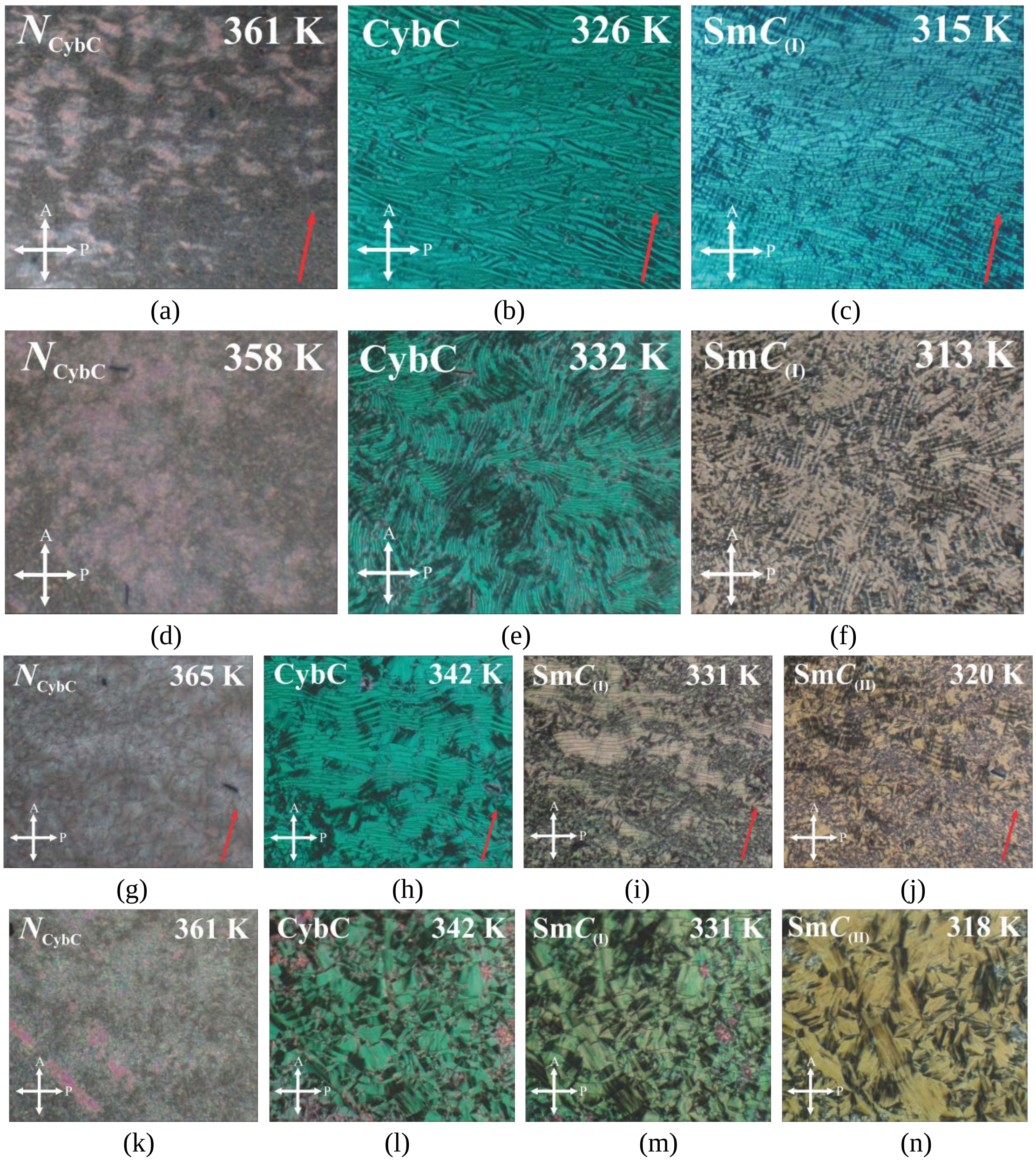

Figure S7. Optical textures of the compound **1/9** and **1/10** for an applied square wave AC voltage at different mesophases; (a-c): compound **1/9** in HG cell, (d-f): compound **1/9** in HT cell, (g-j): compound **1/10** in HG cell, (k-n): compound **1/10** in HT cell. Crossed arrows indicate the direction of the analyzer and polarizer. Red arrows define the rubbing direction in planar orientations.